# The influence of large scale surface roughness on flow factors

## PLEASE CITE THE PUBLISHED VERSION

## PUBLISHER

Balkantrib'14

## VERSION

AM (Accepted Manuscript)

## PUBLISHER STATEMENT

## LICENCE

## REPOSITORY RECORD

# The Influence of Large Scale Surface Roughness on Flow Factors

Michael LEIGHTON[*], Nicholas MORRIS, Ramin RAHMANI, Homer RAHNEJAT

Wolfson School of Mechanical and Manufacturing Engineering, Loughborough University, UK
[*]Corresponding author: M.Leighton@lboro.ac.uk

***Abstract:*** *The average flow model provides a time efficient way of including surface roughness effects in the Reynolds equation. The generation of flow factors relies upon careful measurement of the continuous surfaces to determine the effect of distributed roughness. The current study focuses on the measurement of crosshatched surfaces and the suitability of measurement procedure for accurate generation of representative flow factors. It is found that previous recommendations for the number of grid points and the area considered underestimates that which is actually required. Recommendations are provided for the necessary topographical measurement resolution as well as the determination of the representative sample area as well as typical number of such required areas.*

***Keywords:*** *Cross-hatch honed surfaces, Flow Factors, Piston ring, Cylinder liner*

## Nomenclature

| | | |
|---|---|---|
| $h$ | – Local surface separation | |
| $h_T$ | – Local surface separation | |
| $\bar{h}_T$ | – Mean local surface separation | |
| $L_x$ | – Bearing length in x direction | |
| $L_y$ | – Bearing length in y direction | |
| $p$ | – Local pressure | |
| $\bar{p}$ | – Mean pressure | |
| $\bar{q}_x$ | – Average flow rate in x direction | |
| $\bar{q}_y$ | – Average flow rate in y direction | |
| $S_a$ | – Arithmetic average of surface variation from mean plane | |
| $S_q$ | – Root mean square of surface variation from mean plane | |
| $S_{sk}$ | – Surface roughness frequency distributions asymmetry (Skewness) | |
| $t$ | – Time dimension variable | |
| $U_1$ | – Sliding speed of surface 1 | |
| $U_2$ | – Sliding speed of surface 2 | |
| $x$ | – Cartesian dimension variable | |
| $y$ | – Cartesian dimension variable | |

*Greek symbols*

| | |
|---|---|
| $\gamma$ | – Surface roughness directionality (Peklenik number) |
| $\eta$ | – Lubricant dynamic viscosity |
| $\lambda$ | – The ratio of the RMS surface roughness and the mean surface separation (Stribeck parameter) |
| $\lambda_x$ | – The surface autocorrelation length in the x direction |
| $\sigma$ | – RMS surface roughness |
| $\sigma_1$ | – RMS surface roughness for surface 1 |
| $\sigma_2$ | – RMS surface roughness for surface 2 |
| $\Phi_{s1}$ | – Shear flow factor for surface 1 |
| $\Phi_{s2}$ | – Shear flow factor for surface 2 |
| $\phi_s$ | – Combined shear flow factor |
| $\phi_x$ | – Pressure flow factor in the x direction |
| $\phi_y$ | – Pressure flow factor in the y direction |

## 1. Introduction

The slow sliding speeds and the momentary cessation of sliding associated with reciprocating motion lead to lack of lubricant entrainment into the contact and thus a diminishing lubricant film. Therefore, under such conditions mixed or boundary regimes of lubrication are expected, where surface topography plays an important role.

Reciprocating motion occur in many engineering conjunctions including the piston-cylinder system. The cylinder liner surface comprises larger-scale features than the typical surface roughness features mainly produced through honing or cross-hatching of the cylinder liner. The development of accurate models of large scale roughness and surface features can potentially lead to improvements in predictive analysis, therefore engineering design and machining parameters for contacting surfaces.

Cross hatch honing of the cylinder liner is common in automotive industry. Through proper use of flow factors within the 2D average flow model representation of Reynolds equation [1-2], it is possible to consider the effect of cross hatched features on the tribological performance of the surface. There has been some disagreement in the literature [1-7] with regard to the number of grid computational points which would be needed for the generation of appropriate flow factors. For instance, Teale and Lebeck [5] used a 26x26 node array whilst Lunde and Tonder [6] used a matrix of 100x100 nodes.

The current study considers the effects of measurement resolution and defined sample area as well as the number of

such chosen areas in order to accurately create flow factors for large scale surface features, such as cross-hatching and honing marks. The use of accurate flow factors can then be extended to the tribological conditions in contacts with Stribeck oil film ratios of less than 5, where the roughness of the surface becomes influential in lubrication performance.

## 2. Theory

The average flow model employs statistical sampling in order to make assumptions about the contact topography, where a deterministic analysis of lubricant flow would be difficult. Representative areas are sampled under specific conditions so that the effect of surface topography upon the different components of flow can be analysed independently. Separate flow conditions due to generated pressure in the direction of entrainment (x-direction) and side-leakage (y-direction) as well as that due to shear at the bounding solid surfaces are obtained. These effects are then quantified and included in the standard Reynolds equation (1) in the form of flow factors. This process yields the average flow equation (2).

$$\frac{\partial}{\partial x}\left(\frac{h_T^3}{12\eta}\frac{\partial p}{\partial x}\right) + \frac{\partial}{\partial y}\left(\frac{h_T^3}{12\eta}\frac{\partial p}{\partial y}\right) = \frac{U_1+U_2}{2}\frac{\partial h_T}{\partial x} + \frac{\partial h_T}{\partial t} \tag{1}$$

$$\frac{\partial}{\partial x}\left(\phi_x\frac{h^3}{12\eta}\frac{\partial \bar{p}}{\partial x}\right) + \frac{\partial}{\partial y}\left(\phi_y\frac{h^3}{12\eta}\frac{\partial \bar{p}}{\partial y}\right) = \frac{U_1+U_2}{2}\frac{\partial \bar{h}_T}{\partial x} + \frac{U_1-U_2}{2}\sigma\frac{\partial \varphi_s}{\partial x} + \frac{\partial \bar{h}_T}{\partial t} \tag{2}$$

The statistical sampling of the surface has certain trends which are common to all discrete sampling of a continuous medium [8]. These show that the closer that the sample represents the actual surface by increasing the sample area and measurement resolution, the more representative the resultant flow factors would be in accurate representation of the contact topography. Improvements to sampling can be made in three ways; firstly by increasing the density of the sampling nodes, secondly by enlarging the sample area and thirdly by using a larger number of such sampled areas. Due consideration is given to these important points in the current method and suitable limits are defined through a study of the types of surface roughness simulated in this manner.

The average flow model relies on the standard Reynolds equation for calculating the flow in the small representative areas and therefore, the assumptions of the Reynolds equation are extended to the average flow method. Further assumptions are made in line with those by Patir and Cheng [2]:

- The lubricant is incompressible
- Viscosity is assumed to be constant (There are no thermal effects in the analysis of the representative bearings)
- There is no cavitation
- There is no lubricant flow at the boundaries of the representative areas
- There is no lubricant flow where contact between the surfaces occurs

As explained in some detail by Patir and Cheng [2], to calculate the flow factors, a numerical solution of Reynolds equation is made for several small flat areas, representing the overall contact surface. These small bearings are then solved to find the pressure distribution under specific conditions which would allow the omission of different terms. For the pressure flow factors the two rough bearings representing the roughness of the two surfaces are considered stationary relative to one another with a pressure gradient in one of the Cartesian directions. This results in no shear flow and, as the pressure gradient is in one of the Cartesian frame of reference (either the x or y) the pressure induced flow in each case can be obtained independently. The pressure gradient can then be applied in the other Cartesian direction to find the remaining pressure flow factor. The pressure flow factors are found by analysing the flow rate in comparison to ideal smooth contacting surfaces with the same extent of separation. The Reynolds equation (1) shows that the flow in the x and y directions can be expressed as:

$$\bar{q}_x = \frac{1}{\Delta y}\int_y^{y+\Delta y}\left(-\frac{h_T^3}{12\eta}\frac{\partial p}{\partial x} + \left(\frac{U_1+U_2}{2}\right)h_T\right)dy \tag{3}$$

$$\bar{q}_y = \frac{1}{\Delta x}\int_x^{x+\Delta x}\left(-\frac{h_T^3}{12\eta}\frac{\partial p}{\partial y}\right)dy \tag{4}$$

The average Reynolds equation (2) shows that the flow in the x and y directions can be expressed as:

$$\bar{q}_x = -\phi_x\frac{h^3}{12\eta}\frac{\partial \bar{p}}{\partial x} + \left(\frac{U_1+U_2}{2}\right)\bar{h}_T + \frac{U_1-U_2}{2}\sigma\phi_s \tag{5}$$

$$\bar{q}_y = -\phi_y\frac{h^3}{12\eta}\frac{\partial \bar{p}}{\partial y} \tag{6}$$

Equating equation (3) with (5) and (4) with (6) allows rearrangement of terms in order to find the pressure flow factors with the cancelation of terms allowed by the imposed boundary conditions, thus:

$$\phi_x = \frac{\frac{1}{\Delta y}\int_y^{y+\Delta y}\left(-\frac{h_T^3}{12\eta}\frac{\partial p}{\partial x}\right)dy}{\frac{h^3}{12\eta}\frac{\partial \bar{p}}{\partial x}} \tag{7}$$

$$\phi_y = \frac{\frac{1}{\Delta x}\int_x^{x+\Delta x}\left(-\frac{h_T^3}{12\eta}\frac{\partial p}{\partial y}\right)dx}{\frac{h^3}{12\eta}\frac{\partial \bar{p}}{\partial y}} \tag{8}$$

These equations allow the calculation of the pressure flow factor for each discretised cross-section of the surface. To calculate the pressure flow factor for the entire contacting surface this must simply be averaged over all the discrete cross-sections.

Calculation of the shear flow factor is more complex as each surface must be considered independently. This allows consideration of the transportation due to roughness in each direction as the sliding implies that each surface is moving relative to the other in the opposite sense. As a result the compound flow factor is calculated from equation (9) where $\Phi_{s1}$ and $\Phi_{s2}$ are found through analysis of each bearing surface independently.

$$\phi_s = \left(\frac{\sigma_1}{\sigma}\right)^2 \Phi_{s1} + \left(\frac{\sigma_2}{\sigma}\right)^2 \Phi_{s2} \tag{9}$$

To find the contribution that each surface makes to the shear flow in the contact, each surface is considered when sliding against an idealised flat plane. During this analysis there is no pressure gradient applied across the representative bearing. As a result, certain terms can be omitted from equations (3) and (5), yielding:

$$\Phi_s = \frac{\frac{2}{L_x L_y}\int_0^{L_x}\int_0^{L_y}\left(-\frac{h_T^3 \partial p}{12\eta \partial x}\right)dydx}{(U_1 - U_2)\sigma} \tag{10}$$

The simulation of several small representative areas can then be averaged to find flow factors for a larger contact. This allows complex systems to be analysed effectively if the underlying assumptions of the method can be realised.

## 3. Previous flow factor analyses

In order to apply the method to real surfaces the limitations of the method must be addressed. Patir and Cheng [1, 2] used a matrix of 25×25 nodal points for their analysis and the measurement resolution was approximately three points per autocorrelation length $\lambda_x$. Harp and Salant [4] increased the array to 96×96 points and specified the same resolution. Further analysis by Harp (2000) [3] suggested that this choice was a suitable resolution. Harp [3] also summarised the grid size, resolution and number of sampled areas considered in various previous studies.

*Table 1: Details of previous studies as given by Harp [3]*

| Previous studies | Grid size | Number of grid points per $\lambda_x$ | Number of statistically identical surfaces |
|---|---|---|---|
| Patir and Cheng [1,2] | 25×25 | 3 | 10 |
| Teale and Lebeck [5] | 26×26 | 4 | 10 |
| Lunde and Tonder [6] | 100×100 | 5 or 10 | 10 |
| Peeken, Knoll, et al. [7] | 80×80 | 14 | 10 |
| Harp (2000) [3] | 96×96 | 3 | 50 |

Considering the resolution in terms of the autocorrelation length, proved to be a suitable measure for generated surfaces with linear autocorrelation functions. However, when real surfaces are used this can no longer be assumed to be the case. Consider a cylinder liner surface with cross-hatching. Then, the nominal roughness can be thought of as comprising the large scale roughness of the deeper grooves and the small scale roughness of the intervening plateaus between the grooves. If an autocorrelation length were to be found, then it would be dominated by the large scale roughness of the grooves and any resolution based on this would not necessarily be sufficient for the representation of roughness on the plateaus. In fact, both the resolution and area must be considered if the method is to be applied to cross-hatched surfaces as sufficiently deeper grooves must be included in order to allow the samples to provide an accurate average of the distance between the deeper grooves. Suitable limits for the resolution and area are considered in this study.

## 4. Deriving flow factors for cross-hatched surfaces

An in-house code was produced to use the Patir and Cheng method in which measured surfaces could be analysed with any specified number of data points. Surface data was taken using an Alicona Infinite Focus Microscope with different resolutions using the different optical magnifications (x5, x10, x20, x50, x100). An area of the array measured was then extracted and modelled in the developed code. Varying the area and resolution such that the central point of the considered surface remains at the mean values of distribution approaches a complete representation of the actual surface. As such a large area becomes more statistically representative of the total area; more nodes show more details of surface gradient. Thus, the generated flow factors are more representative of the actual contacting surface. This must trade-off against the time required to analyse a surface as when more nodes are added, either through increasing area or increasing resolution, they affect the measurement time significantly.
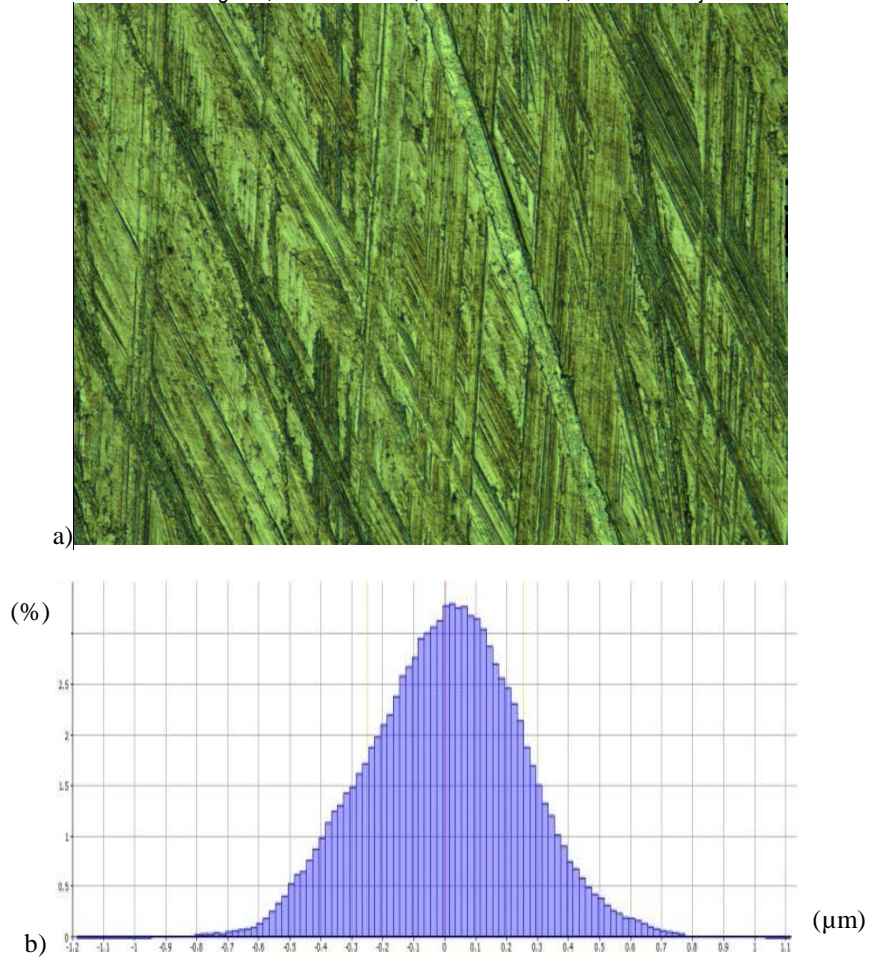
Figure 1: a) Image of a crosshatched cylinder liner at x20 optical magnification (890x675μm) b) Frequency distribution of a cross hatched cylinder liner.

Table 2: Surface roughness parameters for cross hatched cylinder liner

| | |
|---|---|
| $S_a$ | 199.639nm |
| $S_q$ | 251.648nm |
| $S_{sk}$ | 0.0120 |

### 4.1 Sensitivity analysis for measurement resolution

To examine the resultant flow factors as the measurement resolution is varied the surface was imaged with the same centre point but different resolutions. The same area was then analysed numerically for each selected resolution. In figure 2 each line represents a flow factor obtained at the same area, but with a different resolution. It can be seen that pressure flow factors vary considerably where an optical magnification of x5 was used which corresponds to a space of approximately 1.76μm between each node. Applying an autocorrelation function to the surface yields an autocorrelation length of $\lambda_x$=13.882μm. This clearly illustrates the issue with applying Gaussian sampling principles to non-Gaussian surfaces as the resolution is not sufficient for consistent results despite the fact that the resolution is well within the 3points per $\lambda_x$, which is specified by Harp and Salant from Patir and Cheng's work both of whom used Gaussian generated surfaces. It should be noted that cross-hatched cylinder liner surfaces are not Gaussian.

From the graphs it is clear that the pressure flow factors are more closely grouped and have good consistency at x20 resolution and beyond whereas the shear flow factors are closely grouped at x50 and beyond. As a result the x50 optic is used in the current study for data acquisition, which provides a separation of 0.22μm between computational nodes.
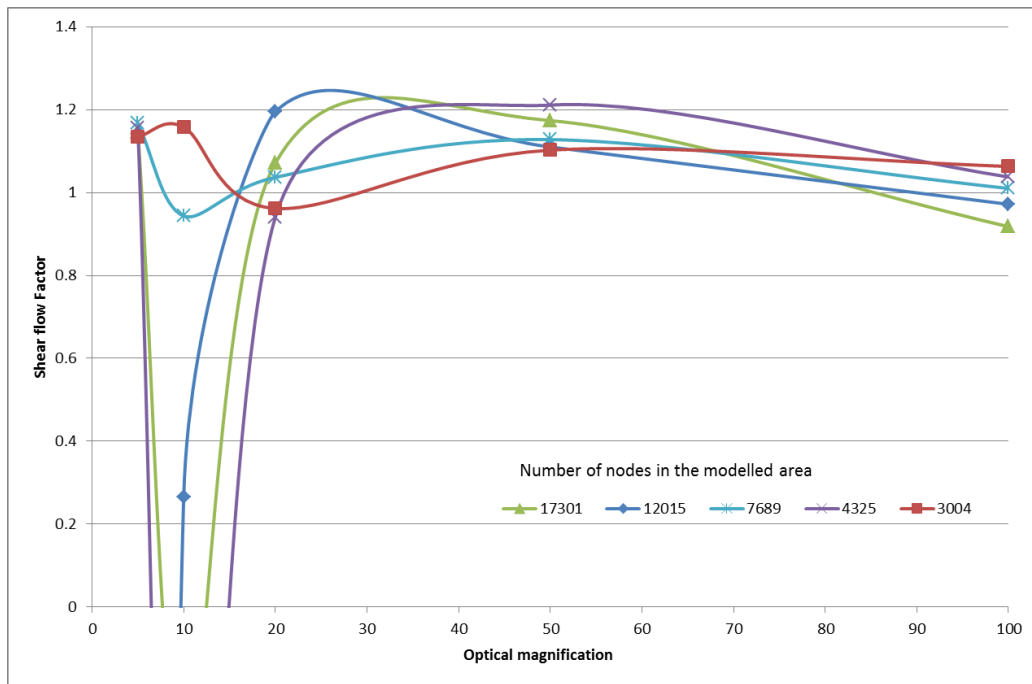
Figure 2 Shear flow factor variation with resolution for different areas
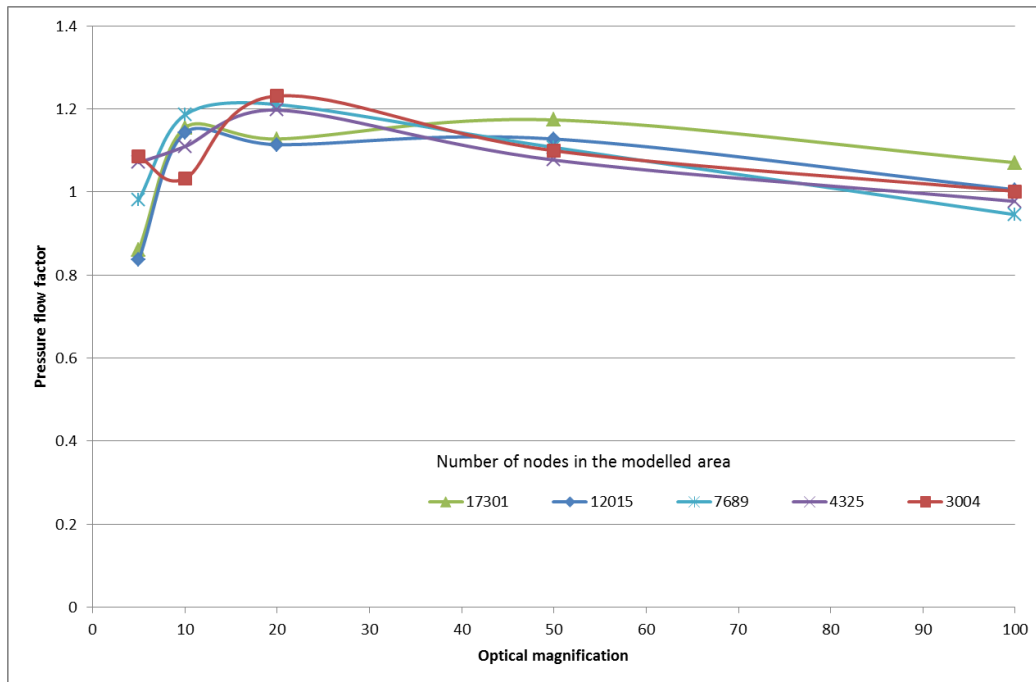


Figure 3 Pressure flow facctor variation with resoloution for different areas

### 4.2 Sensitivity analysis for sample area

As increasing the area or resolution increases the computational time it is desirable to find the minimum area for which the resultant flow factor converges with sufficient accuracy, which with an average of several runs would produce a series of flow factors with small standard deviation and therefore with good agreement.

Pressure and shear flow factors were generated for surfaces with the determined resolution but with different image areas. Plotting the area against the calculated flow factors shows that the results converge as the sample area size is increased. The flow factors are expected to vary as the area changes since there are new surface features included as more nodes are added. However, if the surfaces contain repeatable features, then as the sample area increases the average effect of the surface on the flow converges to the real behavior. This draws attention to some new assumption: Firstly, the surface is repeatable on some scale and secondly that the surface's effects on the lubricant are the same wherever it is sampled on the surface. With the consistency of machining processes and the rigid quality control enforced on high precision components, such as cylinder liners and piston rings, the assumption that the surface is repeatable appears valid and is supported by the findings as the flow factors converge quicker with larger sizes of the sampled area.

The area included in the sample is intrinsically linked with the number of representative bearing surfaces averaged in order to find the flow factor for the overall surface. It is however important to separate the effects of increasing the considered area by averaging more sample bearings and by modelling a larger bearing area for each sample as the boundary conditions set for the representative bearing will have effects within the contact that lessen as the area is

increased due to the distance from the boundaries. Also the area must be sufficient to allow larger scale surface features to be modelled. Therefore the area is set and then more samples are taken and averaged until the resultant average flow factor converges sufficiently.

It may be expected that the larger the area of the representative sample bearings the lower the total sample size would be; however as the sample area size is determined by the size of the surface features and a sufficient number must be considered for the averages to converge the number sampled should be determined by the variability of the surface features, e.g. the depth and spacing of the deeper honing marks.
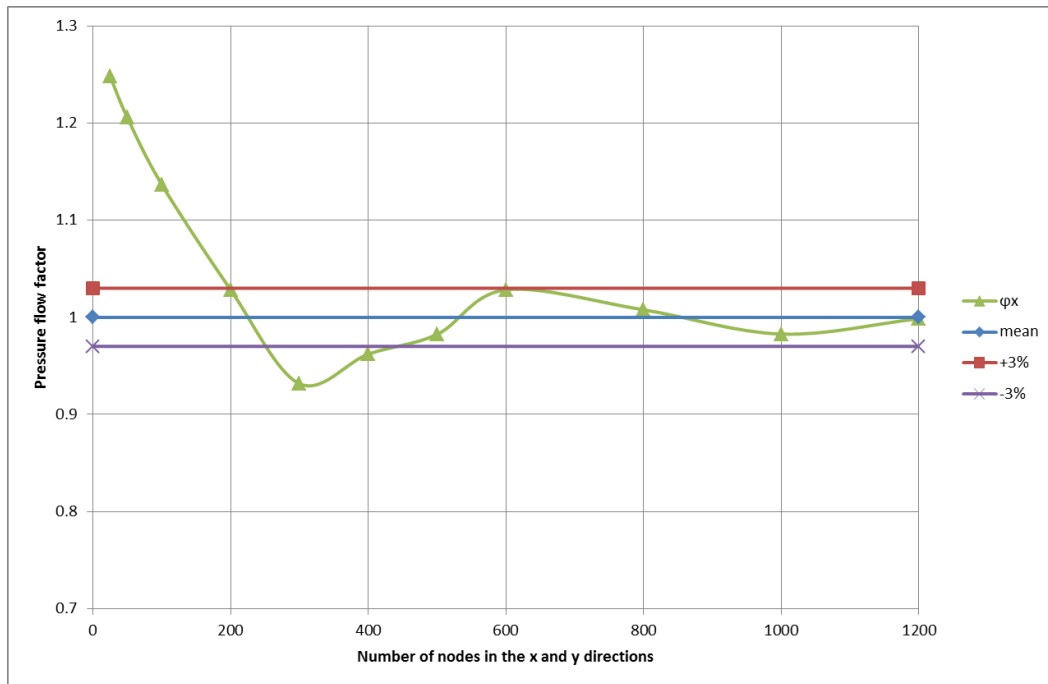


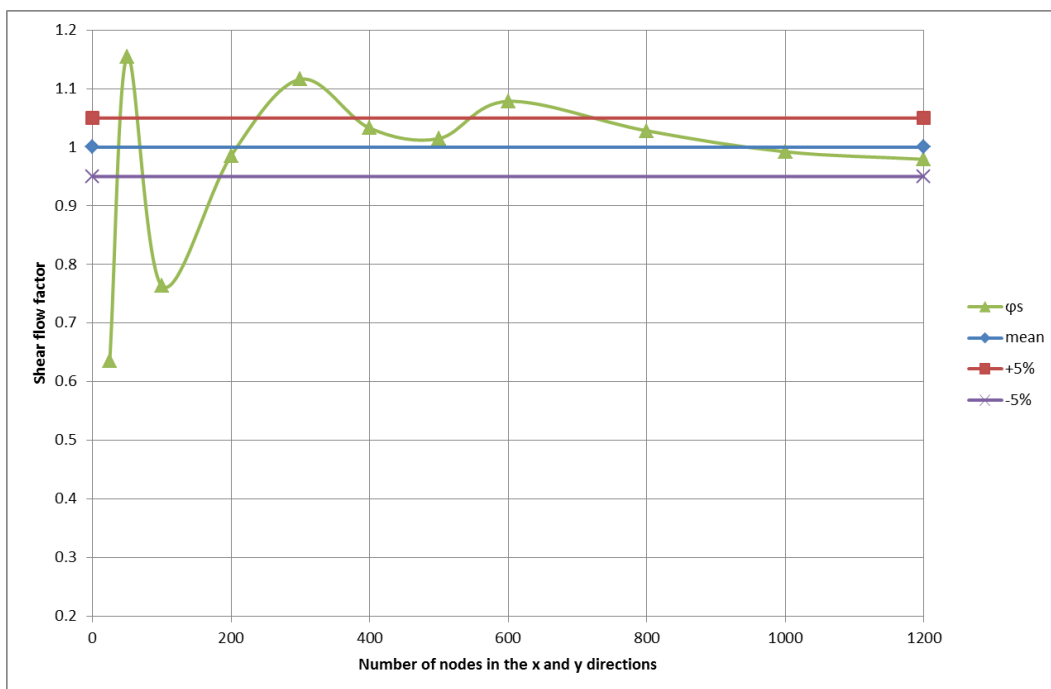*Figure 4 Variation of pressure flow factor with bearing area*



*Figure 5: variation of shear flow factor with bearing area*

Figure 4 shows that the calculated pressure-induced flow factors oscillate and begin to converge for the range of sample area sizes investigated. As the roughness is on a large scale a corresponding large sample area is required before sufficient repeatable features are detected for the resultant flow factors to converge to an almost linear relationship with the sampled area size. However, a completely linear relationship is not necessary as several representative areas will be examined and averaged to find the flow factor. For the pressure flow factors generated in figure 5 this is deemed to be evident for the area with 600 or greater nodal points representation in the x and y directions. For the shear flow factors (figure 6) the same is noted with areas of 800 nodal points in the x and y directions.

### 4.3 Sensitivity analysis for sample number

Using the Alicona IF microscope, measurements of the required area and resolution were taken of a cross-hatched cylinder liner. The generated flow factors were analysed using all the applicable combinations of arithmetic averaging

to find the extent to which they would converge as an increasing number of samples are undertaken. Figure 6 shows that the initial spread in the results is rapidly curtailed as more samples are averaged. The total spread at 8 averaged points is only 0.0609 (approximately ±2.5%). As a result, a sample size of 10 is recommended as this coincides with the number of samples taken in other studies and allows for a close averaging of the data to ensure accuracy in the resulting flow factors.
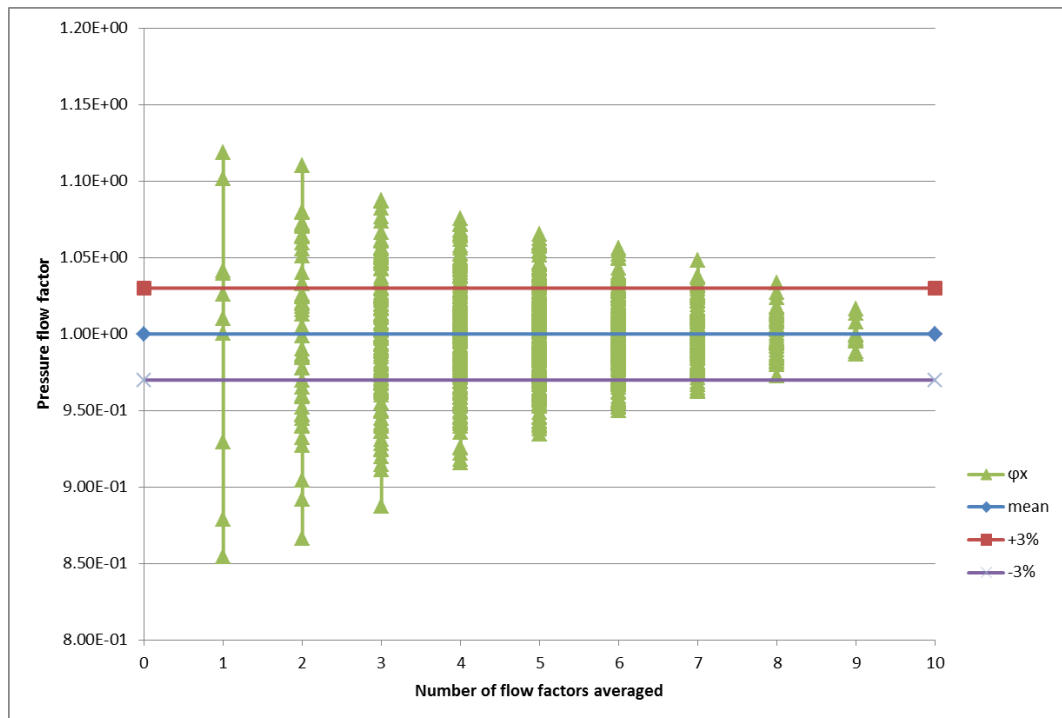


*Figure 6: variation of pressure flow factor average with sample numbers*

## 5. Conclusions

The current study investigates the procedure for the measurement and production of reliable flow factors for non-Gaussian surfaces such as a cross-hatched cylinder liner. These measurements and calculations show that the resolution of the data should have a maximum of 0.22µm inter-spatial nodal distance, with a sampled area of at least 17301µm$^2$ for pressure flow factors (resulting in an array 600x600 points from an image taken with an optical magnification of x50) and 30758µm$^2$ or more for shear flow factors (resulting in an array 800x800 points from an image taken with the same magnification). Finally, there should be at least 10 representative bearing areas averaged to find the flow factors for the surfaces.

## 6. References

[1]   Patir, N., Cheng, H.S., 1978, "An average flow model for determining effects of three-dimensional roughness on partial hydrodynamic lubrication", J. Lubr. Tech., Trans. ASME, 100, pp.12-17
[2]   Patir, N., Cheng, H.S., 1979, "Application of average flow model to lubrication between rough sliding surfaces", J. Lubr. Tech., Trans. ASME, 101, pp.220-230
[3]   Harp, S., "A Computational Method For Evaluating Cavitating Flow" Thesis, Georgia Tec, 2000
[4]   Harp, S R., and R F. Salant. "An average flow model of rough surface lubrication with inter-asperity cavitation." Journal of Tribology 123.1 (2001): 134-143.
[5]   Teale, J. L., and A. O. Lebeck. "An Evaluation of the Average Flow Model [1] for Surface Roughness Effects in Lubrication." Journal of Tribology 102, no. 3 (1980): 360-366.
[6]   Lunde, L., and K. Tonder. "Pressure and shear flow in a rough hydrodynamic bearing, flow factor calculation." Journal of tribology 119, no. 3 (1997): 549-555.
[7]   Peeken, H. J., G. Knoll, A. Rienacker, J. Lang, and R. Schonen. "On the numerical determination of flow factors." Journal of tribology 119, no. 2 (1997): 259-264.
[8]   Whitehouse, D., J. "Handbook of Surface Metrology." Institute of physics, 1994, ISBN 0-7503-0039-6